A Minimum Parameter Adaptive Approach for Rejecting Multiple Narrow-Band Disturbances with Application to Hard Disk Drives

Xu Chen, *Student Member, IEEE,* and Masayoshi Tomizuka, *Fellow, IEEE*

***Abstract*—Many servo systems are subjected to narrow-band disturbances that generate vibrations at multiple frequencies. One example is the track-following control in a hard disk drive (HDD) system, where the airflow-excited disk and actuator vibrations introduce strong and uncertain spectral peaks to the position error signal. Such narrow-band vibrations differ in each product and can appear at frequencies above the bandwidth of the control system. This paper presents a control scheme that adaptively enhances the servo performance at multiple unknown frequencies, while maintaining the baseline servo loop shape. A minimum parameter model of the disturbance is first introduced, followed by the construction of a novel adaptive multiple narrow-band disturbance observer for selective disturbance cancellation. Evaluation of the proposed algorithm is performed on a simulated HDD benchmark problem.**

***Index Terms*—adaptive control, loop shaping, multiple narrow-band disturbances, disks drives**

I. Introduction

In a modern hard disk drive (HDD), data/information is stored in circular patterns of magnetization known as data tracks or simply, tracks. During reading and writing of the data, the disk spins and the read/write head is controlled to follow the circular tracks. This creates the track-following problem, where the servo system performs regulation control to position the read/write head at the desired track, with as low variance as possible. This process is evaluated by the so-called Track Mis-Registration (TMR), which is three times the standard deviation of the position error signal (PES).

One important source of TMR is the vibration/flutter of disks and actuators. This motion is caused by the turbulent air flow within the hard disk assembly or imperfections in the spindle bearing, and results in non-repeatable narrow-band disturbances [1]–[3], whose energy is highly concentrated at multiple unknown frequencies. Due to different operation environments and structures of HDDs, these disturbances differ from track to track and disk to disk. Moreover, frequencies of the narrow-band components can be higher than the bandwidth of the existing servo loop [1], [2]. The above characteristics of such disturbances lead to the difficulty of rejecting them using traditional loop-shaping methods. Similar problems occur in many other systems, such as active suspensions [4], air-forced cooling systems [5], and acoustic systems [6].

Various control algorithms have been developed for narrow-band disturbance rejection. Adaptive Noise Cancellation (ANC) [7] is a very popular feedforward compensation scheme that has been used to reject not only narrow-band vibrations but also wide-band noises. It applies a correlated version of the disturbance (usually measured by additional sensors) to adaptively tune (in general) a Finite Impulse Response (FIR) filter, using Least Mean Squares (LMS) based adaptation algorithms. ANC can be quite effective, and its design principle is simple to realize. Its relative drawbacks are the computation load to adapt a high order FIR filter, the often slow convergence rate to maintain stability, approximations in the LMS convergence proof, and finally the increased cost for sensors, whose precision and bandwidth also greatly determine the compensation quality.

Many more algorithms have been developed in the feedback control category, including: (i) Repetitive Control (RC) and its adaptive versions [8], [9]. (ii) State space design using the Internal Model Principle (IMP) [10], [11]. (iii) Youla Parameterization with an adaptive FIR Q filter [4], [6], [12], [13]. (iv) Adaptive Feedforward Cancellation (AFC) with a Phase-Locked Loop (PLL) [14]. (v) Peak filters [15], [16] and the disturbance observer (DOB) [17], [18]. Among the above algorithms, RC integrates an internal model $1/(1-z^{-N})$ to the closed-loop system, and compensates disturbances at integer multiplications of a base frequency. Internal models for sinusoidal signals, in the forms of differential/difference equations and direct transfer functions, are used in groups (ii) and (iii) to adaptively shape the loop. These IMP based approaches in general do not preserve a baseline loop shape and may change much of the closed-loop dynamics at other frequencies. With the magnitude and the phase responses of the plant (at the disturbance frequencies), AFC with PLL locally performs frequency estimation and disturbance cancellation. Algorithms in [15], [16] selectively increase the loop gain via add-on peak filters, whose coefficients are tuned as functions of the disturbance frequencies. Finally in [17], [18], disturbances are selectively observed

Manuscript received Jan 13, 2011; revised Aug 17, 2011; accepted Oct 26, 2011. This work was supported by the Computer Mechanics Laboratory (CML) in the Department of Mechanical Engineering, University of California, Berkeley.

X. Chen and M. Tomizuka are with the Department of Mechanical Engineering, University of California, Berkeley, CA 94720 USA, e-mails: {maxchen, tomizuka}@me.berkeley.edu

and canceled.

Many of the above mentioned discussions focus on rejecting disturbance with one unknown frequency component, and may not be optimally or directly transformed to the case with multiple bands. Firstly, simple summation of several compensators may not preserve optimality of the sub-compensators. This is particularly true for those in groups (iv) and (v). For instance, in the previous DOB based single narrow-band schemes, merely summing up several band-pass Q filters does not perfectly retain magnitude and phase of each filter at the center frequencies, especially when the frequencies are close to one another or the filters have large bandwidths.[1] Secondly, increasing the frequency components also changes the structure of the parameter adaptation algorithm.

This paper focuses on developing an adaptive feedback control algorithm that rejects multiple narrow-band disturbances at unknown frequencies. A new IMP based adaptive algorithm is constructed to achieve perfect rejection of the interested disturbances. Different from the previous IMP based algorithms which estimate at least $2n$ (n denotes the number of narrow-band components) coefficients, the proposed algorithm adapts only n parameters, which is the minimum requirement to model n general frequency components. Another difference from [4], [6], [10]–[13] is that the proposed algorithm preserves a baseline servo loop shape, and changes little of the system response at the non-interested frequencies. Many of the previous approaches have local parameter convergence or require a white noise condition for global identification. In this paper, new perspectives of online parameter estimation are provided, which involve a two-step adaptation and a corresponding automatic switching algorithm. By such constructions, it is possible to achieve unbiased identification in the noise-free or white noise environments, as well as increased precision for parameter estimation in colored noise situations.

The remainder of this paper is organized as follows. Section II states the problem and the proposed solution. Section III presents the characterization of multiple narrow-band disturbances and the design of the proposed controller structure. The adaptation of the controller parameters is provided in Sections IV and V, after which the efficacy of the method is presented in Section VI. Section VII concludes the paper.

II. The Problem And The Proposed Solution

Fig. 1 shows the proposed block diagram for single-stage HDD track following. It reduces to a general baseline feedback control loop when the dash-dotted box is removed. Throughout the paper we use the open-source HDD benchmark problem [19] as a demonstration tool, which was prepared by a technical committee of IEE Japan, and provides a fourteenth-order plant, denoted as $G_p(z^{-1})$ in Fig. 1, as well as a practical set of input and output disturbances. The transfer function $z^{-m}G_n(z^{-1})$ models the nominal dynamics (at least in the interested frequency range) of $G_p(z^{-1})$. Here the delay term z^{-m} is separated such that the relative degree of $G_n(z^{-1})$ is zero and $G_n(z^{-1})^{-1}$ is thus realizable. The existing feedback controller $C_{FB}(z^{-1})$, designed via any effective loop-shaping algorithm, provides the baseline closed-loop dynamics and yields a sensitivity function with a typical magnitude response as shown in Fig. 2. Notice that a general servo controller has reduced disturbance attenuation capacity as the frequency increases. When energy of the disturbance is concentrated at several unknown frequencies, the baseline controller may easily fail to provide sufficient error rejection.

The reference r is zero in this regulation problem. $d(k)$ and $n(k)$ are respectively the input and the output disturbances. The multiple narrow-band disturbance of interest is lumped in $d(k)$, and lies in the middle and low frequency regions [1], [2].

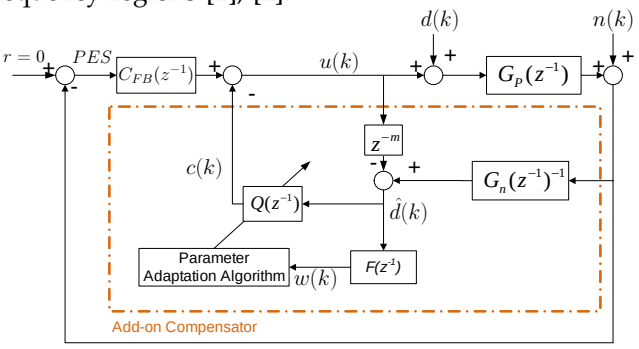

Fig. 1. The structure of the proposed control scheme

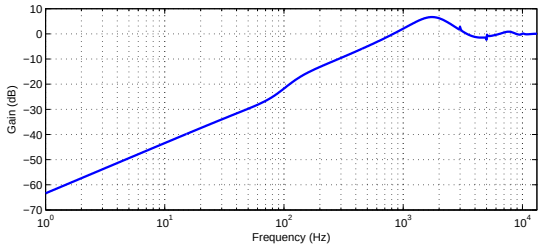

Fig. 2. Magnitude response of a typical sensitivity function

In the proposed compensation scheme, notice first that $\hat{d}(k)$ is given by

$$\hat{d}(k) = G_n(q^{-1})^{-1}\left\{G_p(q^{-1})[u(k)+d(k)]+n(k)\right\} - q^{-m}u(k). \tag{1}$$

Here q^{-1} denotes the one-step delay operator. Throughout this paper, we use q^{-1} for time-domain operation, and z^{-1} for frequency-domain analysis.

In single-stage HDD systems, the nominal plant model has a double-integrator type input/output behavior (to be more exact, the VCM driven actuator also has a friction mode usually below 60 Hz) whose poles and zeros lie inside the unit circle except for one possible zero near $(-1,0)$ on the z-plane. In $G_n(z^{-1})^{-1}$, this nonminimum-phase zero is shifted into the unit circle to create a strictly

[1]Previous DOBs have an additional theoretical limitation, as will be shown in Section II.

stable $G_n(z^{-1})^{-1}$, and to reduce the gains of $G_n(z^{-1})^{-1}$ near the Nyquist frequency. Such modeling does not greatly influence the disturbance rejection performance at frequencies far below the Nyquist frequency. For general mechanical systems, unstable zeros, if any, usually occur in the high frequency region [20], creating no additional difficulty for implementation of the algorithm.

With the stable nominal inverse, if $z^{-m}G_n(z^{-1}) = G_p(z^{-1})$ (i.e. $G_n(z^{-1})^{-1}G_p(z^{-1}) = z^{-m}$), or in regions where the frequency responses of the two transfer functions match, (1) is simplified to

$$\hat{d}(k) = d(k-m) + G_n(q^{-1})^{-1}n(k), \tag{2}$$

i.e. a delayed version of $d(k)$ is contained in $\hat{d}(k)$, with some additional noise.

Processing $\hat{d}(k)$ through a low-pass filter yields a regular disturbance observer (DOB) [21], which however will not provide successful rejection in the narrow-band case. First, due to stability requirements, the bandwidth of the low-pass filter in a regular DOB is quite limited [22] for narrow-band disturbance rejection. Second, the phase of a low-pass filter is not zero but distorted (even within the filter bandwidth), yielding mismatched disturbance cancellation. Finally, the delay m in (2) is not compensated (this is also true in [17], [18]). Such delays can be quite problematic for narrow-band disturbance rejection. For instance, if $m = 1$ and the sampling frequency $F_s = 26400$ Hz, then at 1500 Hz, the one-step delay will introduce $360 \times 1500/F_s = 20.45$ deg of phase mismatch during disturbance cancellation.

From the above discussions, a DOB structure can act to provide magnitude and (shifted) phase information of the narrow-band disturbances. This helps to narrow the design focus to selection of the interested frequency components, and is the reason why the proposed scheme requires just n parameters during adaptation. To correctly extract the signals, a frequency-selection filter $Q(z^{-1})$ is required. For perfect disturbance compensation, such a Q filter also needs to compensate the m-step delay in (2). Through the above signal processing, $c(k)$–the output of $Q(z^{-1})$–"observes" the narrow-band disturbances at unknown frequencies. Substracting $c(k)$ from $d(k)$ in Fig. 1 achieves the disturbance rejection.

By the block-diagram construction in Fig. 1, the steady-state transfer function from $d(k)$ to the position error signal PES is given by

$$G_{d2pes}(z^{-1}) = \left[1 - z^{-m}Q(z^{-1})\right] \times \frac{-G_p(z^{-1})}{1 + C_{FB}(z^{-1})G_p(z^{-1}) + Q(z^{-1})\left[G_n^{-1}(z^{-1})G_p(z^{-1}) - z^{-m}\right]}. \tag{3}$$

When $G_p(z^{-1}) = z^{-m}G_n(z^{-1})$, (3) becomes $G_{d2pes}(z^{-1}) = \frac{-G_p(z^{-1})\left[1-z^{-m}Q(z^{-1})\right]}{1+C_{FB}(z^{-1})G_p(z^{-1})}$, i.e. the add-on compensator shapes the error rejection function in an affine, and thus stable fashion (note that $Q(z^{-1})$ is stable and $G_p(z^{-1})/[1 + C_{FB}(z^{-1})G_p(z^{-1})]$ is the baseline input error rejection function). The closed-loop can thus be shaped by simply designing $1 - z^{-m}Q(z^{-1})$, which depends little on the plant dynamics.

When model uncertainty exists, consider $G_p(z^{-1})$ as a perturbed version of $z^{-m}G_n(z^{-1})$, such that $G_p(z^{-1}) = z^{-m}G_n(z^{-1})[1 + \Delta(z^{-1})]$. We then have

$$G_{d2pes}(z^{-1}) = \frac{-G_p(z^{-1})\left[1 - z^{-m}Q(z^{-1})\right]}{1 + C_{FB}(z^{-1})G_p(z^{-1}) + z^{-m}\Delta(z^{-1})Q(z^{-1})}, \tag{4}$$

from which the closed-loop characteristic polynomial is seen to come from $A_c(z^{-1}) = 1 + C_{FB}(z^{-1})G_p(z^{-1}) + z^{-m}\Delta(z^{-1})Q(z^{-1})$. A sufficient condition for robust stability is therefore: $\forall\ \omega$, $\left|e^{-jm\omega}\Delta(e^{-j\omega})Q(e^{-j\omega})\right| < \left|1 + C_{FB}(e^{-j\omega})G_p(e^{-j\omega})\right|$, i.e.

$$\left|Q(e^{-j\omega})\right| < \left|\frac{1}{S_o(e^{-j\omega})\Delta(e^{-j\omega})}\right|, \tag{5}$$

where $S_o(e^{-j\omega}) \triangleq 1/[1 + C_{FB}(e^{-j\omega})G_p(e^{-j\omega})]$ is the frequency response of the baseline sensitivity function.

III. Q-filter Design

A. The Internal Models of the Disturbance

From the nature of the vibrations, the multiple narrow-band disturbance can be modeled as the sum of several sinusoidal signals [1], [2]. Consider the general form of

$$w(k) = \sum_{i=1}^{n} C_i \sin(\omega_i k + \psi_i), \tag{6}$$

where n is the number of frequency components, ω_i's are the unknown frequencies,[2] C_i's and ψ_i's are the corresponding unknown magnitudes and phases. To construct a well-defined problem, we assume that: (i) C_i is real and nonzero; (ii) $k \geq 0$ and $\omega_i \neq \omega_j$. In this subsection, it is assumed that n is known (indeed in HDDs, the number of major disk/actuator modes are usually available). Discussions on how to identify n will be provided in Section V.

When $n = 1$, it is easy to see that, after two time steps of transient response, a single sinusoidal signal satisfies,

$$\left(1 - 2\cos(\omega)q^{-1} + q^{-2}\right)C\sin(\omega k + \psi) = 0,\ \forall k \geq 2, \tag{7}$$

where $1/(1 - 2\cos(\omega)q^{-1} + q^{-2})$ is known as the internal model [23] of a single sinusoid. Extending (7) to the case of multiple frequency components, we have

$$\prod_{i=1}^{n}\left(1 - 2\cos(\omega_i)q^{-1} + q^{-2}\right)w(k+1) = 0,\ \forall k \geq 2n-1. \tag{8}$$

For verification of (8) in the frequency domain, one can easily show that $\forall\omega_i$, $A(e^{-j\omega_i}) \triangleq \prod_{i=1}^{n}(1 - 2\cos(\omega_i)e^{-j\omega} + e^{-2j\omega})\big|_{\omega=\omega_i} = 0$, which indicates that any periodic input to $A(z^{-1})$, at the frequency ω_i, will yield null output at the steady state.

[2] $\omega_i = 2\pi\Omega_i T_s$, where Ω_i is in Hz, and T_s is the sampling time.

Define the new variables a_i's that satisfy

$$A(q^{-1}) = \prod_{i=1}^{n} \left(1 - 2\cos(\omega_i)q^{-1} + q^{-2}\right) \tag{9}$$

$$= 1 + \sum_{i=1}^{n-1} a_i(q^{-i} + q^{-2n+i}) + a_n q^{-n} + q^{-2n}, \tag{10}$$

where in the second equality we have used the fact that coefficients of 1 and q^{-2} are the same in $1-2\cos(\omega_i)q^{-1}+q^{-2}$. We have thus obtained in (9) and (10) nonlinear and linear (in parameters) internal models of multiple narrow-band disturbances. Each model is determined by only n parameters, which is the minimal possible number for n general sinusoidal signals [23].

B. Internal Model Based Q-filter Design

Recalling the transfer function from $d(k)$ to PES in (4), and noting that in the interested frequency region an accurate plant model is available, we have

$$PES(k) \approx \frac{-G_p(q^{-1})}{1 + C_{FB}(q^{-1})G_p(q^{-1})} \cdot \left[1 - q^{-m}Q(q^{-1})\right] d(k). \tag{11}$$

Consider the general case that $d(k)$ is composed of n narrow-band components, and that $Q(z^{-1})$ is a stable infinite impulse response (IIR) filter given by $Q(z^{-1}) = B_Q(z^{-1})/A_Q(z^{-1})$. A sufficient condition to regulate PES to zero is

$$\left[1 - q^{-m}\frac{B_Q(q^{-1})}{A_Q(q^{-1})}\right] d(k) = 0. \tag{12}$$

By applying now the internal model derived in the previous subsection, (12) can be achieved if

$$q^{-m}B_Q(q^{-1}) = A_Q(q^{-1}) - J(q^{-1})A(q^{-1}), \tag{13}$$

where $A(q^{-1})$ is given by (10), and $J(q^{-1})$ is a polynomial to be assigned shortly.

A stable band-pass structure is proposed for $Q(z^{-1})$ to have the previously mentioned frequency-selection ability. A natural assignment for $A_Q(z^{-1})$ is

$$A_Q(z^{-1}) = \prod_{i=1}^{n} \left(1 - 2\alpha\cos\omega_i z^{-1} + \alpha^2 z^{-2}\right), \tag{14}$$

which provides $Q(z^{-1})$ pairs of poles at $\alpha e^{\pm\omega_i}$ $(i = 1, \ldots, n)$, and hence the emphasis of the input to $Q(z^{-1})$ at ω_i's. As α approaches 1, the passband becomes sharper and the transient response of $Q(z^{-1})$ becomes longer.[3]

By construction, (9), (10), and (14) are connected by:

$$A_Q(z^{-1}) = A(\alpha z^{-1}) = 1 + a_1\alpha z^{-1} + \cdots + a_n\alpha^n z^{-n} + \cdots + a_1\alpha^{2n-1}z^{-2n+1} + \alpha^{2n}z^{-2n}. \tag{15}$$

[3]Specifically, due to (14), the impulse response of $Q(z^{-1})$ is the summation of decaying sinusoidals, with the decay rate at time step k governed by α^k. It takes approximately $\lfloor 1/\log(\alpha^{-1}) \rfloor$ ($\lfloor\cdot\rfloor$ denotes the closest integer value) samples for the impulse response to settle to 37 percent ($\approx e^{-1}$) of its peak value.

With $A(q^{-1})$ in (10), $A_Q(q^{-1})$ in (15), and q^{-m} from the nominal plant, (13) can be ordered as $J(q^{-1})A(q^{-1}) + q^{-m}B_Q(q^{-1}) = A_Q(q^{-1})$, which is a Diophantine equation. Solving this polynomial equation (for $B_Q(q^{-1})$ and $J(q^{-1})$) is similar to performing pole placements, where $A_Q(q^{-1})$ is the fictitious closed-loop characteristic polynomial, and q^{-m} and $A(q^{-1})$ come from the numerator and denominator of a fictitious plant. Since q^{-m} and $A(q^{-1})$ are coprime, the solution is unique if

$$\deg\left(A_Q(q^{-1})\right) \le \deg\left(B_Q(q^{-1})\right) + m,$$
$$\deg\left(B_Q(q^{-1})\right) + m = \deg\left(J(q^{-1})\right) + \deg\left(A(q^{-1})\right).$$

In the HDD example, $m = 1$. The minimum order solution to (13) is: $J(q^{-1}) = 1$, and

$$B_Q(q^{-1}) = \sum_{i=1}^{2n} (\alpha^i - 1)a_i q^{-i+1},\ a_i = a_{2n-i},\ a_{2n} = 1. \tag{16}$$

Solutions for $m > 1$ can be similarly derived, in which case $\deg\left(J(q^{-1})\right)$ will no longer be 0.

Remarks:

- When $m > 1$, and $\deg\left(J(q^{-1})\right) \neq 0$, (13) indicates that the proposed compensator is additionally capable to reject disturbances with the internal model $1/J(q^{-1})$.
- To introduce extra properties to the compensator, one can pre-assign fixed zeros to $Q(z^{-1})$, e.g. at $z = -1$, such that at the Nyquist frequency $Q(e^{-j\pi}) = 0$. To achieve this, one need to solve

  $$\left[q^{-m}(1 + q^{-1})\right]\tilde{B}_Q(q^{-1}) = A_Q(q^{-1}) - J(q^{-1})A(q^{-1})$$

  to get a final Q filter given by $Q(z^{-1}) = \frac{(1+z^{-1})\tilde{B}_Q(z^{-1})}{A_Q(z^{-1})}$, where the $1 + z^{-1}$ part enforces additional gain reduction at high frequencies.
- Using (13), one can verify that at any center frequency ω_i of the Q filter,

  $$Q(e^{-j\omega_i}) = \left.\frac{z^m\left(A_Q(z^{-1}) - J(z^{-1})A(z^{-1})\right)}{A_Q(z^{-1})}\right|_{z=e^{j\omega_i}} = e^{jm\omega_i},$$

  where the last equality was due to the proved result $A(e^{-j\omega_i}) = 0$ in Section III-A. We have thus obtained a causal Q filter that selects the multiple narrow-band signals in $d(k)$ and provides exactly m-step phase advances to compensate the delays in (2).

IV. The Parameter Adaptation Algorithm

The center frequencies of the proposed Q filter are determined by the n parameters a_i's. In this section, an adaptive algorithm is developed to estimate these quantities. The proposed adaptation starts with the pre-filter $F(z^{-1})$ in Fig. 1. As shown in Section II, $\hat{d}(k)$, the input to $F(z^{-1})$, estimates the non-measurable disturbance. $F(z^{-1})$ is proposed to be the nominal version of $-G_p(z^{-1})/\left(1 + C_{FB}(z^{-1})G_p(z^{-1})\right)$, i.e. the negative of the input error rejection function, so that the output of $F(z^{-1})$,

denoted as $w(k)$, reflects the baseline PES.[4] Additional low-pass or band-pass filtering can be incorporated to improve the signal-to-noise ratio for the direct adaptive control algorithm in this section.

A. The Adaptation Model and the Predictor

The proposed Parameter Adaptation Algorithm (PAA) aims at applying an adaptive IIR $\hat{Q}(q^{-1})$ such that $\left[1-q^{-m}\hat{Q}(q^{-1})\right]w(k)$ is minimized in the presence of multiple unknown narrow-band disturbances. The adaptation is not standard, since for the $2n$-order filter $Q(z^{-1})$, the number of adaptation parameters is just n. From (13) and (15), one can obtain $1-q^{-m}Q(q^{-1}) = J(q^{-1})\frac{A(q^{-1})}{A(\alpha q^{-1})}$. Since our focus is the narrow-band disturbances with the internal model $1/A(z^{-1})$, the $J(q^{-1})$ part can be removed from the PAA (in the HDD benchmark, no removal is necessary since $m=1$ and $J(q^{-1})=1$). Therefore the adaptation model is $y(k) \triangleq \frac{A(q^{-1})}{A(\alpha q^{-1})}w(k)$, which is equivalent to

$$A(\alpha q^{-1})y(k) = A(q^{-1})w(k). \tag{17}$$

Applying (10) and (15), one can obtain the following difference equation of (17)

$$y(k) = \psi(k-1)^T\theta + w(k) + w(k-2n) - \alpha^{2n}y(k-2n), \tag{18}$$

where $\theta \triangleq [a_1, a_2, \ldots, a_n]^T$ is the unknown parameter vector, and the regressor vector $\psi(k-1)\left(\triangleq [\psi_1(k-1), \psi_2(k-1), \ldots, \psi_n(k-1)]^T\right)$ satisfies

$$\begin{aligned}\psi_i(k-1) &= w(k-i) + w(k-2n+i) \\ &\quad - \alpha^i y(k-i) - \alpha^{2n-i}y(k-2n+i); \quad i = 1, \ldots, n-1,\end{aligned} \tag{19}$$

$$\psi_n(k-1) = w(k-n) - \alpha^n y(k-n). \tag{20}$$

Replacing $A(q^{-1})$ and $A(\alpha q^{-1})$ by their adaptive versions, and denoting the corresponding output by $e(k)$, one obtains the adaptive system

$$\hat{A}\left(\alpha q^{-1}, \hat{\theta}(k)\right)e(k) = \hat{A}\left(q^{-1}, \hat{\theta}(k)\right)w(k), \tag{21}$$

whose difference equation is given by

$$e(k) = \phi(k-1)^T\hat{\theta}(k) + w(k) + w(k-2n) - \alpha^{2n}e(k-2n). \tag{22}$$

Here $\hat{\theta}(k)$ is the estimate of θ; $\phi(k-1)$ consists of

$$\begin{aligned}\phi_i(k-1) &= w(k-i) + w(k-2n+i) \\ &\quad - \alpha^i e(k-i) - \alpha^{2n-i}e(k-2n+i); \quad i = 1, \ldots, n-1,\end{aligned} \tag{23}$$

$$\phi_n(k-1) = w(k-n) - \alpha^n e(k-n). \tag{24}$$

Our aim is to have a recursive update in the form of $\hat{\theta}(k) = \hat{\theta}(k-1) + $Error Correction. For an ideal $Q(q^{-1})$, as shown in Section III-B, the steady state of $y(k)$ equals zero. One can thus note that $e(k)$ and $\hat{\theta}(k)$ are respectively the *a posteriori* estimation error and the *a posteriori* parameter estimate. Replacing $\hat{\theta}(k)$ by $\hat{\theta}(k-1)$ in (22) gives the *a priori* estimation error:

$$e^o(k) = \phi(k-1)^T\hat{\theta}(k-1) + w(k) + w(k-2n) - \alpha^{2n}e(k-2n). \tag{25}$$

The application of *a posteriori* information in (25) is essential for adaptation in noisy environments. Notice that $e(k)$ is more accurate than $e^o(k)$, since the former is updated by a more recent $\hat{\theta}(k)$. Notice also that the incorporation of $e(k-i)$, $i = 0, 1, \ldots 2n$ in (22) and (25) would not be achievable if $Q(z^{-1})$ had been chosen as an FIR filter.

In this paper we apply the PAA using the output error predictor with a fixed compensator, due to its simplicity and good performance in noisy environments (see, for example, [24]). The idea is to apply $\nu(k) = C(q^{-1})e(k)$, a filtered version of $e(k)$ as the adaptation error, to update $\hat{\theta}(k)$ (in the *a posteriori* sense). The fixed compensator $C(q^{-1})$ is proposed to be given by

$$\begin{aligned}C(q^{-1}) = 1 + c_1\alpha q^{-1} + \cdots + c_n\alpha^n q^{-n} + \\ \cdots + c_1\alpha^{2n-1}q^{-2n+1} + \alpha^{2n}q^{-2n},\end{aligned} \tag{26}$$

i.e. by replacing every a_i in $A(\alpha q^{-1})$ by c_i.

The *a posteriori* adaptation error $\nu(k)$, and the (implementable) *a priori* adaptation error $\nu^0(k)$, are therefore

$$\nu(k) = e(k) + \alpha^{2n}e(k-2n) + \varphi(k-1)^T\theta_c, \tag{27}$$

$$\nu^o(k) = e^o(k) + \alpha^{2n}e(k-2n) + \varphi(k-1)^T\theta_c, \tag{28}$$

where from (26), we have

$$\begin{aligned}\theta_c &= [c_1, c_2, \ldots, c_n]^T, \\ \varphi(k-1) &= [\varphi_1(k-1), \varphi_2(k-1), \ldots, \varphi_n(k-1)]^T, \\ \varphi_i(k-1) &= \alpha^i e(k-i) + \alpha^{2n-i}e(k-2n+i); \; i = 1, \ldots, n-1, \\ \varphi_n(k-1) &= \alpha^n e(k-n).\end{aligned}$$

Estimation of $\hat{\theta}(k)$ can now be performed through the following PAA:

$$\hat{\theta}(k) = \hat{\theta}(k-1) + \frac{P(k-1)\left(-\phi(k-1)\right)\nu^o(k)}{1 + \phi(k-1)^T P(k-1)\phi(k-1)}, \tag{29}$$

$$P(k) = \frac{1}{\lambda(k)}\left[P(k-1) - \frac{P(k-1)\phi(k-1)\phi^T(k-1)P(k-1)}{\lambda(k) + \phi^T(k-1)P(k-1)\phi(k-1)}\right], \tag{30}$$

where $P(k)$ is the adaptation gain; the negative sign in $-\phi(k-1)$ in (29) is due to the update in the negative direction of the cost gradient; $\lambda(k) \in [0,1]$ is the forgetting factor designed based on stationarity of the process and the required adaptation speed [25]. In this paper, $\lambda(k) = 1 - 0.99 \times (1 - \lambda(k-1))$ with $\lambda(0) = 0.97$.

To apply (29)-(30), one first computes $e(k)$ and $e^o(k)$ from (22) and (25), and then obtains $\nu^o(k)$ from (28).

Due to the fact that the more accurate *a posteriori* $e(k)$ is used in the direct adaptation, the above PAA maintains good performance when the adaptation input $w(k)$ contains noise. The algorithm is subjected to the

[4] Alternatively, to reduce computation (at the sacrifice of some performance), one may first freeze the compensator, use directly the PES for parameter adaptation, then turn on compensation after parameter convergence.

following sufficient stability condition [24]: the transfer function

$$\frac{C(z^{-1})}{A_Q(z^{-1})} - \frac{1}{2} \tag{31}$$

is strictly positive real (SPR).

If $C(z^{-1})$ is close to $A_Q(z^{-1})$, (31) is approximately 1/2, and thus SPR. The structural design of (26) was due to this reason. It now remains to choose the values of the compensator coefficients θ_c. If knowledge of the narrow-band disturbances, such as the statistical mean of the frequencies, is available, $C(z^{-1})$ can directly be assigned using (9), (10), (15), and (26). If no such knowledge can be obtained, the series-parallel predictor proposed in the following subsection can be applied as an initialization horizon, to get an approximate version of $A_Q(z^{-1})$ for $C(z^{-1})$. The series-parallel predictor is computationally simplified, always stable, and actually provides unbiased estimation when the adaptation input is noise free [24].

B. Initialization Horizon with a Series-Parallel Predictor

Recalling the adaptation model in (18), if we do not use the *a posteriori* term $e(k)$ but only replace θ by $\hat{\theta}(k-1)$, the parameter estimate at time $k-1$, we get the *a priori* prediction of $y(k)$ and the corresponding *a priori* prediction error $\epsilon^o(k)$:

$$\hat{y}^o(k) = \psi(k-1)^T \hat{\theta}(k-1) + \Big(w(k) + w(k-2n) - \alpha^{2n} y(k-2n)\Big), \tag{32}$$

$$\epsilon^o(k) = y(k) - \hat{y}^o(k). \tag{33}$$

$\epsilon^o(k)$ is applied as the adaptation error in this series-parallel predictor. Note from our central design criteria, that for a tuned $Q(q^{-1})$, the ideal output $y(k)$ is zero at the steady state. This observation simplifies the regression vector to

$$\psi_i(k-1) = w(k-i) + w(k-2n+i); \quad i = 1, \ldots, n-1, \tag{34}$$

$$\psi_n(k-1) = w(k-n), \tag{35}$$

and the estimation error in (33) now becomes

$$\epsilon^o(k) = -\psi(k-1)^T \hat{\theta}(k-1) - (w(k) + w(k-2n)). \tag{36}$$

With the above information, the following RLS type PAA can be constructed:

$$\hat{\theta}(k) = \hat{\theta}(k-1) + \frac{P(k-1)\psi(k-1)\epsilon^o(k)}{1 + \psi(k-1)^T P(k-1)\psi(k-1)}, \tag{37}$$

$$P(k) = P(k-1) - \frac{P(k-1)\psi(k-1)\psi(k-1)^T P(k-1)}{1 + \psi(k-1)^T P(k-1)\psi(k-1)}. \tag{38}$$

When parameters have converged for the above PAA, the value of $\hat{\theta}$ is applied to initialize $C(z^{-1})$ and $\hat{Q}(z^{-1})$. During the initialization horizon, it is advised not to apply disturbance compensation, due to possible large parameter variations. It will be shown later in Section VI, that this transient period is actually quite small.

C. Dynamic Switching Between Two Predictors

This section discusses how to connect the two PAAs in Sections IV-B and IV-A. Conventionally, switching between two sets of predictors is usually done by choosing a fixed transition time instant. As for the confirmation of parameter convergence, common choices are to monitor either the adaptation gain or the adaptation error. For the former case, since the adaptation gain $P(k)$ is in general a matrix, some operation such as taking the trace is needed to judge the size of $P(k)$. For the latter, monitoring the adaptation error is well-suited for processes with high signal-to-noise ratio. However, when the parameters are biased or the adaptation algorithm has local convergence, it is difficult to decide the threshold for convergence. This paper proposes an algorithm to automate the switching. We directly focus on the values of the parameter estimate $\hat{\theta}(k)$, and regard it to have converged if

1) $\max\Big(|\delta\hat{\theta}(k)|\Big) \triangleq \max\Big(|\hat{\theta}(k) - \hat{\theta}(k-1)|\Big) < \epsilon$, where ϵ is a pre-defined tolerance.
2) condition 1) holds continuously for a number of samples.

Note that ϵ is directly related to the parameters and is much easier to choose than the threshold of the adaptation gain or that of the adaptation error. One can remark that the proposed algorithm is an approximation of the Cauchy criterion [26].

V. Other Practical Aspects

Determining the Number of Narrow-band Components: It is always beneficial to apply as much engineering experience as possible to obtain a close estimation of n, the number of narrow-band disturbances. If indeed no information on n is available, several *series-parallel* predictors in Section IV-B, with different filter orders, can be run simultaneously in the initialization horizon. Comparing the respective estimation errors, one can then choose the algorithm which is fastest at reducing $e(k)$ to a level comparable to the disturbance-free case.

Transforming between parameters: Equations (9) and (10) represent respectively filters in the cascade and the direct forms. If a_i's in (10) are obtained, ω_i's in (9) can be obtained by calculating the roots of $A(q^{-1})$. Equation (10) has been mainly used for direct controller design. Equation (9) is useful for analysis, e.g. to check the disturbance frequency and the performance of PAA.

VI. Case Studies

The proposed compensation scheme was implemented in the simulated HDD benchmark problem [19]. The baseline control system was as shown in Section II. Except the repeatable runout (which is always pre-compensated in practice), all common disturbances and measurement noises were included in the simulation. The sampling time, the spindle rotation speed, and the track density are respectively 3.788×10^{-5} sec, 7200 rpm,

and 100,000 Tracks Per Inch. In all case studies, the shaping coefficient α in $Q(z^{-1})$ increased from 0.95 to 0.995 for fast transient response and good steady-state performance.

Two narrow band disturbances at 500 Hz and 1200 Hz were injected at the end of the first revolution. The upper plot in Fig. 3 shows the time trace of the position error signals without compensation. The corresponding steady-state frequency spectrum is plotted in the dotted line in Fig. 4. We can see that without compensation, the PES had strong energy components at 500 Hz and 1200 Hz; the TMR was 21.56% Track Pitch (TP). Notice that 1200 Hz is higher than the bandwidth of the baseline servo system. Without compensation, disturbance at this frequency was amplified.

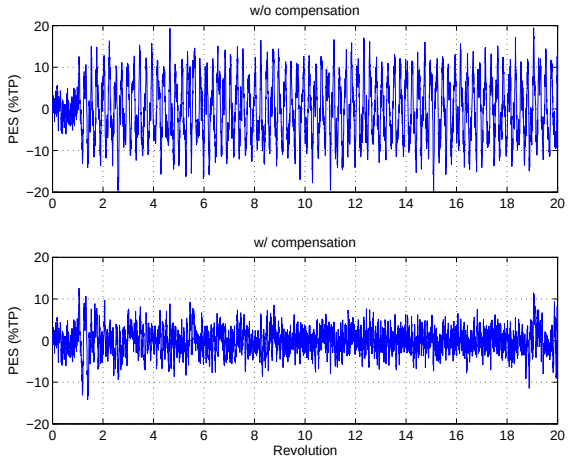

Fig. 3. Time traces of PES with and without compensation

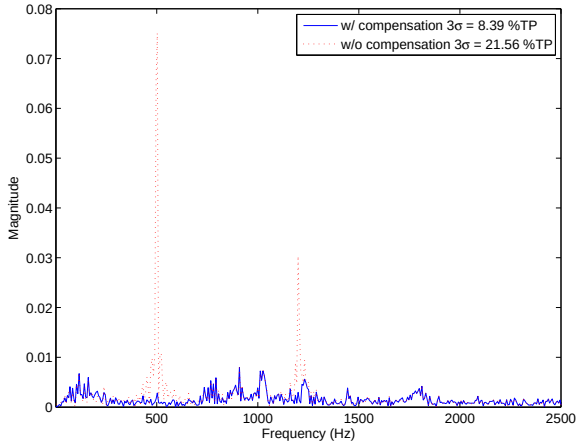

Fig. 4. Frequency spectra of PES with and without compensation

The proposed algorithm was applied to improve the servo performance. An online fault detector that computed TMR in a moving window of 20 samples, was utilized to detect the disturbance. The parameter adaptation was initialized at 700 Hz, by using (9) and (10). Fig. 5 shows the identified disturbance frequencies (computed off-line from the a_i's). After disturbance detection, the series-parallel predictor was automatically turned on at 1.25th revolution. The dynamic switching algorithms then operated to find a continuous 30-sample window where all online identified coefficients did not have abrupt changes in values. At around 1.48th revolution, the series-parallel predictor automatically switched to the more accurate parallel predictor, and the disturbance compensation was turned on. Note that in this case study, the 30-sample window for convergence detection was intentionally made conversative, to visually demonstrate the convergence speed between the two vertical lines in Fig. 5.

The frequency- and time-domain compensation results are shown in Figs. 6, 4, and 3. After convergence, the closed-loop sensitivity function had the frequency response as shown in the dotted line of Fig. 6. Correspondingly in Fig. 4, the major narrow-band components were fully attenuated, while the frequency spectra in other regions were hardly influenced. In the time domain, the lower plot in Fig. 3 demonstrates the PES time trace with compensation, where we note the PES dropped to be significantly below 10% TP. The corresponding TMR (after convergence) was reduced to 8.39% TP–less than one half of the value without compensation.

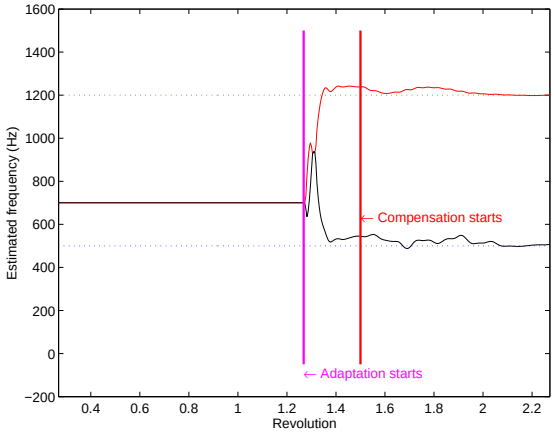

Fig. 5. Adaptive identification of two frequencies at 500 and 1200 Hz

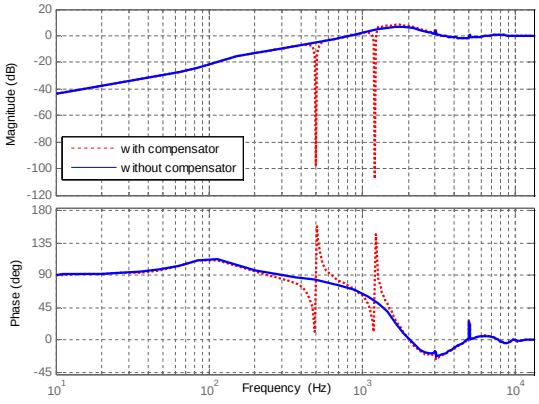

Fig. 6. Frequency responses of the sensitivity functions with and without compensation

Fig. 7 and Fig. 8 show the performance of the algorithm at higher frequencies and with the parameters initialized far away from their true values. Notice that

in this case study, more small spectral peaks appear as input noise to the PAA (see Fig. 7), yet the algorithm found and fully rejected the two major disturbance components.

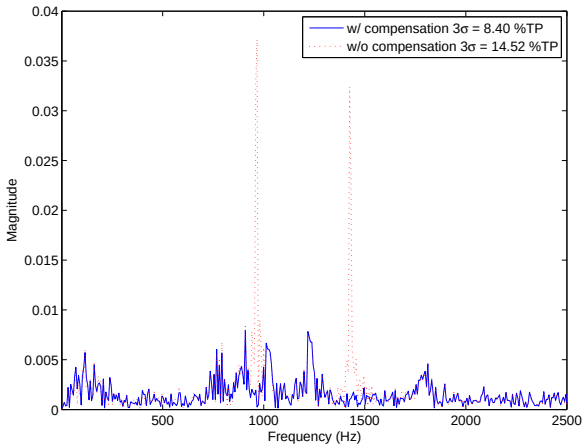

Fig. 7. Frequency spectra of PES with and without compensation: the case for two narrow-band disturbances at 964 Hz and 1426 Hz

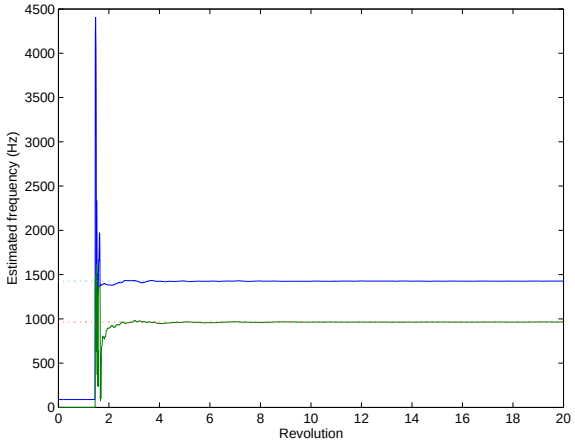

Fig. 8. Identification of two frequencies at 964 Hz and 1426 Hz

VII. Conclusion

In this paper, an adaptive control scheme was proposed to reject multiple narrow-band disturbances with application to HDD track following. Simulations on a realistic open-source HDD benchmark problem showed that the proposed algorithm significantly reduced PES and TMR. The proposed method is suitable for compensating multiple disturbances with narrow peaks in the frequency spectrum.

References

[1] L. Guo and Y. Chen, "Disk flutter and its impact on HDD servo performance," in *Proceedings of 2000 Asia-Pacific Magnetic Recording Conference*, 2000, pp. TA2/1–TA2/2.

[2] R. Ehrlich and D. Curran, "Major HDD TMR sources and projected scaling with TPI," *IEEE Transactions on Magnetics*, vol. 35, no. 2, pp. 885–891, 1999.

[3] J. McAllister, "The effect of disk platter resonances on track misregistration in 3.5 inch disk drives," *IEEE Transactions on Magnetics*, vol. 32, no. 3, pp. 1762–1766, May 1996.

[4] I. D. Landau, A. Constantinescu, and D. Rey, "Adaptive narrow band disturbance rejection applied to an active suspension–an internal model principle approach," *Automatica*, vol. 41, no. 4, pp. 563–574, Apr. 2005.

[5] C. Kinney, R. de Callafon, E. Dunens, R. Bargerhuff, and C. Bash, "Optimal periodic disturbance reduction for active noise cancelation," *Journal of Sound and Vibration*, vol. 305, no. 1-2, pp. 22–33, Aug. 2007.

[6] F. Ben-Amara, P. T. Kabamba, and a. G. Ulsoy, "Adaptive sinusoidal disturbance rejection in linear discrete-time systems–part II: Experiments," *ASME Journal of Dynamic Systems, Measurement, and Control*, vol. 121, no. 4, pp. 655–659, 1999.

[7] B. Widrow, J. Glover Jr, J. McCool, J. Kaunitz, C. Williams, R. Hearn, J. Zeidler, E. Dong Jr, and R. Goodlin, "Adaptive noise cancelling: principles and applications," *Proceedings of the IEEE*, vol. 63, no. 12, pp. 1692–1716, 1975.

[8] M. Steinbuch, "Repetitive control for systems with uncertain period-time," *Automatica*, vol. 38, no. 12, pp. 2103–2109, 2002.

[9] C. Li, D. Zhang, and X. Zhuang, "A survey of repetitive control," in *Proceedings of 2004 IEEE/RSJ International Conference on Intelligent Robots and Systems*, vol. 2, Jan. 2004, pp. 1160 – 1166.

[10] W. Kim, H. Kim, C. Chung, and M. Tomizuka, "Adaptive output regulation for the rejection of a periodic disturbance with an unknown frequency," *IEEE Transactions on Control Systems Technology*, vol. 19, no. 5, pp. 1296–1304, 2011.

[11] Q. Zhang and L. Brown, "Noise analysis of an algorithm for uncertain frequency identification," *IEEE Transactions on Automatic Control*, vol. 51, no. 1, pp. 103–110, 2006.

[12] R. de Callafon and C. E. Kinney, "Robust estimation and adaptive controller tuning for variance minimization in servo systems," *Journal of Advanced Mechanical Design, Systems, and Manufacturing*, vol. 4, no. 1, pp. 130–142, 2010.

[13] F. Ben-Amara, P. T. Kabamba, and a. G. Ulsoy, "Adaptive sinusoidal disturbance rejection in linear discrete-time systems–part I: Theory," *ASME Journal of Dynamic Systems, Measurement, and Control*, vol. 121, no. 4, pp. 648–654, 1999.

[14] M. Bodson and S. C. Douglas, "Adaptive algorithms for the rejection of sinusoidal disturbances with unknown frequency," *Automatica*, vol. 33, no. 12, pp. 2213 – 2221, 1997.

[15] Y.-H. Kim, C.-I. Kang, and M. Tomizuka, "Adaptive and optimal rejection of non-repeatable disturbance in hard disk drives," in *Proceedings of 2005 IEEE/ASME International Conference on Advanced Intelligent Mechatronics*, 2005, pp. 1–6.

[16] J. Zheng, G. Guo, Y. Wang, and W. E. Wong, "Optimal narrow-band disturbance filter for PZT-actuated head positioning control on a spinstand," *IEEE Transactions on Magnetics*, vol. 42, no. 11, pp. 3745–3751, 2006.

[17] Q. Zheng and M. Tomizuka, "A disturbance observer approach to detecting and rejecting narrow-band disturbances in hard disk drives," in *Proceedings of 2008 IEEE International Workshop on Advanced Motion Control*, 2008, pp. 254–259.

[18] Q.-W. Jia, "Disturbance rejection through disturbance observer with adaptive frequency estimation," *IEEE Transactions on Magnetics*, vol. 45, no. 6, pp. 2675–2678, 2009.

[19] IEEJ, Technical Commitee for Novel Nanoscale Servo Control, "NSS benchmark problem of hard disk drive systems," http://mizugaki.iis.u-tokyo.ac.jp/nss/, 2007.

[20] S. Skogestad and I. Postlethwaite, *Multivariable Feedback Control: Analysis and Design*, 2nd ed. Wiley Chichester, UK, 2005.

[21] K. Ohnishi, "Robust motion control by disturbance observer," *Journal of the Robotics Society of Japan*, vol. 11, no. 4, pp. 486–493, 1993.

[22] M. White, M. Tomizuka, and C. Smith, "Improved track following in magnetic disk drives using a disturbance observer," *IEEE/ASME Transactions on Mechatronics*, vol. 5, no. 1, pp. 3–11, 2000.

[23] B. Francis and W. Wonham, "The internal model principle of control theory," *Automatica*, vol. 12, no. 5, pp. 457–465, 1976.

[24] I. D. Landau, R. Lozano, and M. M'Saad, *Adaptive Control*. Springer-Verlag New York, Inc., 1998.

[25] L. Ljung, *System Identification: Theory for the User*, 2nd ed. Prentice Hall PTR, 1999.

[26] W. Rudin, *Principles of Mathematical Analysis*. McGraw-Hill New York, 1976, vol. 275.